IEEE Access
Multidisciplinary ⋮ Rapid Review ⋮ Open Access Journal

Received 5 June 2024, accepted 2 July 2024, date of publication 4 July 2024, date of current version 12 July 2024.

Digital Object Identifier 10.1109/ACCESS.2024.3423653

RESEARCH ARTICLE

Frequency-Difference Electrical Impedance Imaging of Cervical Specimens

TAWEECHAI OUYPORNKOCHAGORN[1], (Senior Member, IEEE), NAPATSAWAN NGAMDI[1], SAIROONG OUYPORNKOCHAGORN[2], JARUWAN SRIWILAI[3], AND THERDKIAT TRONGWONGSA[3]

[1]Faculty of Engineering, Srinakharinwirot University, Nakhon Nayok 26120, Thailand
[2]Faculty of Science, Naresuan University, Phitsanulok 65000, Thailand
[3]Faculty of Medicine, Srinakharinwirot University, Nakhon Nayok 26120, Thailand

Corresponding author: Taweechai Ouypornkochagorn (taweechai@g.swu.ac.th)

This work was supported by the Research Fund from Srinakharinwirot University.

This work involved human subjects or animals in its research. Approval of all ethical and experimental procedures and protocols was granted by the Human Research Ethical Committee of Srinakharinwirot University under Reference No. SWUEC-097/2563.

ABSTRACT Screening for cervical abnormalities is crucial to reduce the risk of developing abnormal cells in the cervix. Several pathological methods have been proposed to date, however, they require exhaustive histological examination and time. In this paper, we proposed a method to localize the abnormality by using reconstruction images. The weighted frequency-difference Electrical Impedance Tomography (WfdEIT) method was implemented on three cervical specimens: one normal, one with Cervical intraepithelial neoplasia (CIN) grade 2, and one cancer specimen. A 16-electrode probe was developed to work with an EIT system operated at 2-125 kHz excitation frequencies. Experimental results have shown that the abnormalities in the specimens could be identified in most cases, represented by the positive conductivity changes. The localization of the CIN2 specimen was more accurate than that of the cancer specimen. The conductivities of the transformation zone (TZ) part and the cancer region of the specimens were significantly higher than those of the ectocervical part by 1.5-2.2 times. Interestingly, the tissue in the TZ part had a similar frequency spectrum of conductivity to the tissue with cancer and this caused difficulty to distinguish between them. The TZ region of the specimens in the reconstruction images was always positive in conductivity change in a similar manner to cancer. The abnormality imaging for identifying cancer in the TZ region is then still challenging.

INDEX TERMS Cervix, cervical specimens, loop electrosurgical excision procedure (LEEP), weighted frequency-difference electrical impedance tomography (WfdEIT), conductivity, reconstruction.

I. INTRODUCTION

Cervical cancer is an abnormal growth of cells on the surface of the cervix. The abnormality could be specific to different stages of Cervical intraepithelial neoplasia (CIN) or the most severe stage i.e. cancer. CIN development can be categorized into three grades: grade 1 (CIN1), grade 2 (CIN2), and grade 3 (CIN3) which is the most severe one. The cervix could be divided into three parts. The Endocervix is the inner part of the cervix. The epithelium in this part consists of columnar cells lining from the external orifice (the cervical canal) to the uterus. The Ectocervix is the outer part covered by a stratified squamous epithelium. The last part is the region where the squamous epithelium transforms to the columnar epithelium which is called the transformation zone (TZ) residing near the orifice. The epithelium is the mixture of squamous, columnar, or cuboidal cells. The abnormal cells usually arise in this TZ part [1], [2].

Screening for cervical abnormalities could be in vivo or in vitro. Colposcopy is a visual inspection method using an

The associate editor coordinating the review of this manuscript and approving it for publication was Md. Moinul Hossain.

endoscope. The detectability of this method was reported at 30-70% [3]. The inspected cervices need to be washed with the acetic acid solution first to turn the abnormal tissue into white. Papanicolaou (Pap) smear test is the most popular pre-screening method by taking some epithelium cells into a certain pathological process before investigating with a microscope. This method is simple, but the detectability was reported at only 55.4% [4]. Liquid-based cytology (LBC) and human papillomavirus (HPV) DNA testing with reflex cytology are methods that could increase the detectability to 89.5% and 94%, respectively [4]. Pathological cell suspension and HPV DNA detection process are required in these methods. Investigating cervical specimens obtained from the loop electrosurgical excision procedure (LEEP) method can provide accurate pathological results. This method is brought to verify the presence of abnormality that is usually conducted during the treatment or at the late stage of investigation [5]. Sectioning and slide preparation processes are required for examining LEEP specimens, and the experience of pathologists is also essential with this method [6].

Cervical abnormalities cause changes in the shape of cervical cells and the structure of the cell lining where the significance of the change depends on the abnormality grade. Due to the change of the cells, the presence of abnormality could be reflected by the electrical conductivity of cervical smears in suspension or cervices. Reference [7] reported that the conductivity of abnormal smears was 166 times higher than that of normal smears at the 10-kHz excitation frequency. However, the in vivo conductivity of CIN1-CIN3-grade tissues was only 4.7-5.2 [6] or 1.25-2.5 times [8] higher than the conductivity of normal cervices at the same frequency – much smaller than what was found in smears. These conductivities were higher at the high frequencies [6], [7], [8], [9]. For example, in the case of normal cervices/ smears, the conductivity at 10 kHz increased by 5 [7], 6.25 [8], or 2.3 [9] times at 100 kHz. However, in the case of abnormal cervices/ smears, it increased by 2 [7] or 1.8-5 times [8] – smaller than that of normal cervices/ smears. These different characteristics then have been used for distinguishing normal and abnormal cervices/ smears. Actually, the use of conductivity for determining the changing state of measured objects/bodies has been reported in other biomedical applications as well. For example, [10] reported the use of conductivity to monitor the porosity and the swelling ratio of tissue scaffolds. Reference [11] also proposed a similar way to monitor the change of urine in bladders.

The conductivity measurement could be conducted by using a well-chamber (for the smear case) [7], an electrode probe [6], [8], [9], [12], [13], [14], [15], [16], a tube [17], or a planar electrode plate [18]. Fixing excitation current of 2-219 μArms [6], [9], [12], [13] or fixing supply voltage of 10 $mV_{peak-peak}$ [7] at the frequency of 100 Hz-1 MHz has been implemented. Principally, the four-electrode method was used to estimate the conductivity. In the case of the electrode probe, the number of electrodes in a probe could be 4-16 electrodes. References [6], [8], [12], and [9] proposed a four-electrode probe with 5.5 mm in diameter of the electrode array, that arranged into a square shape. The diameter of each electrode was 1 mm in diameter. Eight measurement sites were conducted to determine the conductivity. Reference [19] proposed a seven-electrode probe with a 3-mm diameter electrode array. The diameter of electrodes was 0.9 mm. Reference [15] proposed an eight-electrode probe arranged into two rings (3 mm in diameter for the inner ring containing four 0.6 mm-diameter electrodes, and 5.5 mm in diameter for the outer ring containing four 1.5 mm-diameter electrodes.) References [13] and [14] proposed a 16-electrode probe arranged into two rings with 0.9-1 mm diameter electrodes. The diameter of the inner ring was 4.2 mm for [13] and 6.67 mm for [14], while that of the outer ring was 7 mm for [13] and 10 mm for [14].

Apart from determining the existence of abnormality in a cervix with conductivity, imaging conductivity distribution is another method that can be used for addressing the abnormality. The image could provide more information that helps in diagnosis, planning the treatment, or pathological examination. Electrical Impedance Tomography (EIT) is a potential technique for creating an image of conductivity distribution by using the voltage information obtained from the surface of a measuring tissue after applying a small excitation current. This technique is fast and simple for measurement. EIT has been used in many medical applications e.g. lung and brain applications [20], [21]. Traditional EIT is a time-difference basis (tdEIT) that requires measurement at a reference period first. This is practically difficult in many medical applications, including the cervix application, as measurements on healthy cervices must be conducted beforehand. Frequency-difference EIT is later proposed based on the fact that each tissue has its own frequency spectrum of conductivity [22]. Measurement data at high and low frequencies, at the same measurement time, are chosen for reconstruction. The conductivity difference of the selected frequencies is displayed in the reconstruction image, and the abnormality will show up in the image if the frequency spectrums of conductivity are different from that of normal tissues. The measurement data at the healthy state is then not necessary. Several devised frequency-difference EIT methods were proposed in the past, however, they are generally based on two methods [16], [23]. First, the simple frequency-difference EIT method (called here ''fdEIT method'') is the most basic one that uses the high-frequency measurement data as the reference state. The conductivity difference of tissues is imaged. However, since the conductivity change (between the high- and the low-frequency) occurs in the whole volume, the fdEIT method is then suitable only in a homogeneous condition. Second, the weighted-fdEIT method (called here ''WfdEIT method'') is a modified version that creates new reference data by projecting the vector of the low-frequency measurement to that of the high-frequency measurement [16], [23], [24]. The conductivity change of the background volume could be reduced,

FIGURE 1. Measurement system.

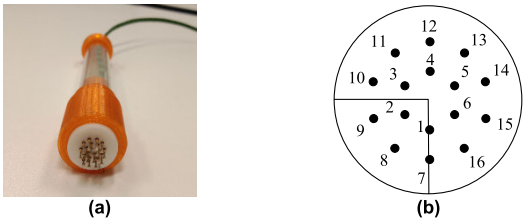

FIGURE 2. Measurement probe (a) and the electrode layout (b). The radial lines presented in the layout are the position markers used in Fig. 12-Fig. 14.

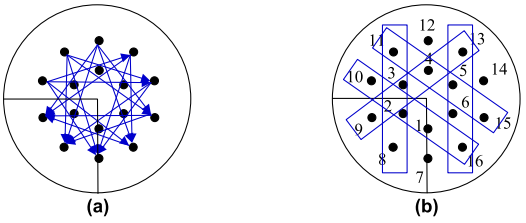

FIGURE 3. Current patterns (a) and the selection composite measurements used for determining tissue conductivity (in the blue rectangle boxes).

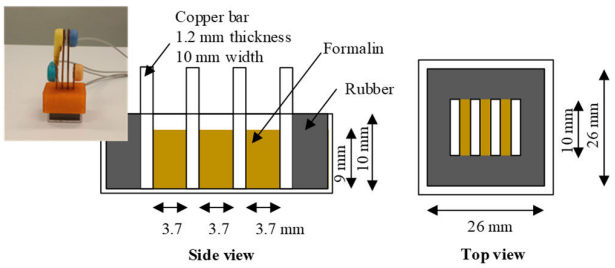

FIGURE 4. Chamber used for measuring the conductivity of formalin.

and then it could improve the reconstruction performance. However, the abnormality to be reconstructed should not be too large in volume.

EIT has not been reported often for reconstructing the conductivity distribution within a small volume that is compatible with the size of cervices or cervical specimens. Reference [25] reported to use of 15-mm diameter-well chambers with a 16-electrode configuration for localizing cell-loaded hydrogel in liquid solution. The fdEIT method was implemented based on a pair of 10 kHz and 100 kHz. The hydrogel could be clearly detected in this study. Reference [16] proposed to use a 16-electrode probe of 20 mm in electrode array diameter to reconstruct for abnormality of a whole cervical specimen. The simulation and the phantom experiment were conducted with this probe, and the result showed that both the fdEIT and the WfdEIT methods could localize the abnormality even though the noise was present.

In this study, the conductivities of cervical specimens in different parts were investigated. The conductivity distribution of cervical specimens was also imaged with the frequency-difference EIT technique. A small 16-electrode probe was developed for these purposes. Three cervical specimens were carefully selected in the investigation. The pathological examination reports were used for verification of the reconstruction results. To our knowledge, this is the first report of the frequency-difference image of the conductivity distribution of cervix specimens. This could reveal the possibility of using the image to address the abnormality of cervical specimens. This paper is organized as follows: the next section explains the method to measure the boundary voltages, calculate the conductivity, reconstruction, and experiment with cervical specimens. The results of the reconstruction algorithm investigation, measured conductivities, and reconstruction images of cervical specimens are in Section III. The discussion is made in Section IV, and the final section is devoted to the conclusion.

II. METHODS

A. MEASURING SYSTEM

The Clementine EIT system was used in this study [26] (Fig. 1). A series of five stimulation currents of 2, 10, 25, 50, and 125 kHz was injected at the same moment, and the measurement data of each frequency was simultaneously collected. Due to the small size of the measured specimens, the amplitudes were programmed to 50 μArms at 2 kHz, 200 μArms at 10 kHz, and 400 μArms at 25, 50, and 125 kHz. The recording speed was 20 frames/s. The signal-to-noise (SNR) ratio of the system was reported at 91.7 dB for the voltage measurement unit and 78.5 dB for the current source unit. The system was supported to measure with 32 channels, but only 16 channels were used in this study. A 16-electrode probe with a 20 mm-diameter head was developed (Fig. 2a). The pin electrodes were arranged into two rings: 3.6 mm and 6.8 mm in diameter for the inner ring and the outer ring, respectively (Fig. 2b). The number of electrodes for the inner and the outer ring was 6 and 10, respectively. Each electrode was with a support spring helping in firm contact with the measured specimens. Twenty excitation current patterns were programmed as in Fig. 3a. The adjacent voltage measurement scheme was selected. For example, when the current is injected from Electrode#14 to #7, the voltage measurement will be performed on Electrode#1 and #2, #2 and #3, and so on. The total number of composite measurements then was 240. Five measurements were selected for determining the local conductivity of measured tissues as shown in Fig. 3b i.e. Electrode#10-#16: #1-#2, #8-#11:#2-#3, #9-#13:#3-#4,

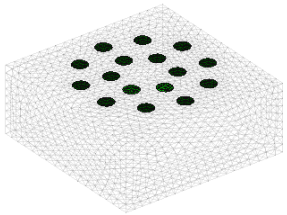

FIGURE 5. Cervix model that was used for determining the correction factor in (1) and for image reconstruction.

#11-#15:#4-#5, and #13-#16:#5-#6 (displayed in a format of "current electrode pair:voltage measurement electrode pair".)

The measurement voltages obtained from the probe were used for imaging the abnormality in the specimens and for determining the conductivity of the different parts of the cervical specimens. However, since the specimens were fixated in 10% neutral buffered formalin beforehand, the conductivity of formalin was investigated in this study as well. A plastic chamber was developed with the size of 29 × 29 × 27 mm (Fig. 4). Four copper bars were used as the electrodes. The amplitudes of the excitation were the same as those used in the measurement with the developed probe.

B. CONDUCTIVITY ESTIMATION OF TISSUES AND FORMALIN

The conductivity estimation used in this study was based on the four-point measurement. Ideally, the electrodes are required to be equally separated by distance s and aligned into a straight line. In the case of the measurement with the probe where the electrodes have to be on the specimen surface, the estimation can be estimated by (1) where σ is the estimated conductivity, I is the excitation current, V is the measurement voltage, and t is the specimen's thickness [19], [27]. The estimation in [27] assumes that the electrode distance is much larger than the electrode diameter, however, this condition was not met in this study. The contact area of electrodes could also affect the estimation, and then the correction factor α was added into (1), following what was proposed in [19]. Considering the selected five measurements mentioned in Section II-A, the inner electrode pair was not straightly aligned to the outer electrode pair (Fig. 3b). The correction factor was then not only used for compensating the influence of the electrode area in this study but it also was used for compensating the misaligned of the electrodes in this study. To obtain α, a simulation situation was created. A finite-element model of cervical specimens was created with 10 × 10 × 4 mm in size (Fig. 5). The number of elements was 33,344. The contact impedance was set to 0.01 Ω and the simulation current was 400 μArms. The conductivity of the cervical tissue was set to 0.1, 0.2, 0.3, 0.4, and 0.5 S/m. The electrode distance s, however, was determined by the distance between the outer electrodes divided by three. The value of α in (1) that fit the estimation to the simulation conductivities over the selected five measurements was examined.

$$\sigma = \alpha \cdot \frac{I}{V\pi t} \cdot \left(\ln\left(sinh\left(\frac{t}{s}\right) \cdot \left(sinh\left(\frac{t}{2s}\right)\right)^{-1}\right)\right) \quad (1)$$

In the case of formalin conductivity estimation, the estimation was determined by (2) where A is the area of the copper bars that contacted the formalin solution in the chamber. Since the formalin solution was filled in the chamber with a height of 9 mm, therefore, regarding the size of the chamber and the copper bar (Fig. 4), the area A was 90 mm^2.

$$\sigma = \frac{I}{V} \cdot \frac{A}{s} \quad (2)$$

C. IMAGE RECONSTRUCTION

Image reconstruction based on the frequency-difference EIT (fdEIT) used in this study is a mathematical process to generate a tomographic image that displays the difference in tissue conductivity (σ) of two different frequencies. Two voltage measurements operated at the different excitation frequencies are required i.e. $V_{freq-low}$ and $V_{freq-high}$, where $V_{freq-low}$ is of low frequencies and $V_{freq-high}$ is of high frequencies. Since the tissue conductivity of high frequencies is usually higher than that of low conductivity and tends to have lower sensitivity to the presence of tissue abnormality, $V_{freq-high}$ is usually used as the reference frequency [16], [23], [24]. The conductivity distribution at the low frequency (*freq-low*) is estimated by (3) where U is the discretization modeling function. Tikhonov regularization method as in (4) is used to solve (3) where $\Delta\tilde{\sigma}$ is the different distribution between that of the low and the high frequency, J is the sensitivity matrix, R is the prior information, and λ is the regularization parameter [16], [23]. We called this reconstruction method the "fdEIT" method (the simplest method.) This method was reported that suitable for a homogeneous and frequency-invariant background [16], [24].

$$\hat{\sigma} = \arg\min_{\sigma} \left\{ \left\| V_{freq-low} - U(\sigma) \right\|^2 \right\} \quad (3)$$

$$\Delta\tilde{\sigma} = \left(J^T J + \lambda R^T R \right)^{-1} J^T \left(V_{freq-low} - V_{freq-high} \right) \quad (4)$$

The so-called weighted-fdEIT (called here the "WfdEIT" method) is an improved version of the fdEIT method. The new reference voltage is generated by projecting $V_{freq-low}$ to $V_{freq-high}$ as in (5) and (6) [19], [23]. The conductivity distribution of the WfdEIT method is estimated by (7). The WfdEIT method has been widely implemented with multifrequency EIT systems due to the high tolerance of background variation.

$$V_{freq-low,proj} = \alpha V_{freq-high} \quad (5)$$

$$\alpha = \left(V_{freq-low} \cdot V_{freq-high} \right) / \left\| V_{freq-high} \right\|^2 \quad (6)$$

$$\Delta\tilde{\sigma} = \left(J^T J + \lambda R^T R \right)^{-1} J^T \left(V_{freq-low} - V_{freq-low,proj} \right) \quad (7)$$

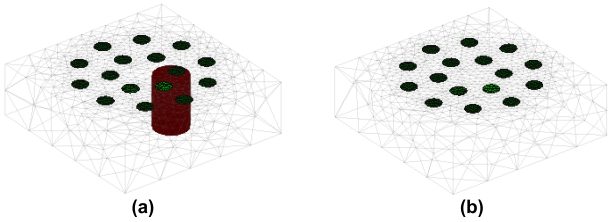

FIGURE 6. Forward cervix model (a) and inverse cervix model (b) that were used for investigating the performance of the fdEIT and the WfdEIT reconstruction methods.

In this study, the Regularized Newton-Krylov Generalized Minimal Residual (GMRes) method was used for the reconstruction shown in (4) and (7) [19], [23], [28]. The number of Krylov subspaces was 200 and the smoothness prior was selected for R. The regularization parameter was assigned to 1×10^{-7}. The modeling function was computed by using the EIDORS software [29]. The fdEIT and the WfdEIT methods were investigated by simulation first. Two dual cervix models of the same size as the model mentioned in Section II-B were created for this purpose (Fig. 6). The forward model contained 9,777 elements having a cylindrical abnormality with 2 mm in diameter. The homogeneous inverse model contained 9,267 elements. The conductivity of the low-frequency and that of the high-frequency of the normal region were set to 0.067 S/m and 0.213 S/m, respectively. The conductivity of the low-frequency and the high-frequency of the abnormal region were set to 0.347 S/m and 0.442 S/m, respectively. These conductivities were based on the conductivity of normal cervical tissues and CIN2 tissues at 10 kHz and 50 kHz reported in [6]. It is worth noting that only the WfdEIT method was implemented for the image reconstruction of the specimens (regarding the simulation result.) The fine model used in Section II-B was used in this reconstruction task (Fig. 5).

D. SPECIMENS AND INVESTIGATION PROCEDURE

Three cervical specimens obtained from three patients obtained from the Loop Electrosurgical Excision Procedure (LEEP) method were investigated in this study (Table 1). The specimens were taken out and later kept in 10% neutral buffered formalin for four hours before being brought into the pathological examination. Gross examination was conducted by a pathologist, and the measurements with the Clementine EIT system were next performed. After the measurements, a regular pathological examination was carried out. Each specimen was cut at every 30 degrees where the orifice was the center (Fig. 7). The number of section tissues was then 12. The section tissues were mounted in cassettes and later brought to the process of making slides for microscopic examination. The spreading region of abnormality (if it is present) was investigated from these section tissues by a microscope and by an experienced pathologist. The reconstruction images of the un-sectioned specimens were created first, and the pathological results were brought for validation

TABLE 1. Summary of cervical specimen diagnoses.

Specimen	Size (mm)	Morphology	Diagnosis
A	10x15x4	Very soft, large region of the orifice	Cancer with 2-4 mm in thickness
B	12x15x4	Hard, very small region of the orifice	CIN2 with 1.7-3 mm in thickness
C	15x20x4	Soft, large region of the orifice	Normal

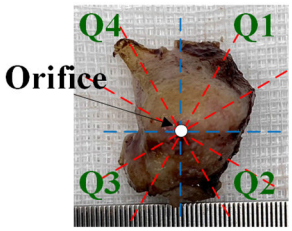

FIGURE 7. Cutting sites of cervical specimens.

FIGURE 8. The measurement on the surface of the cervical specimens.

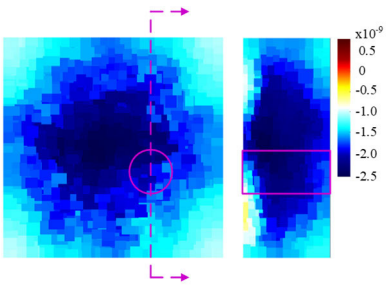

FIGURE 9. The reconstruction images obtained with the fdEIT method. The left image is the top view and the right image is the side view. The magenta circle (in the left image) and the magenta rectangle (in the right image) indicate the true location of the abnormality.

next. The experiment procedure has been prior approved by the Human Research Ethical Committee of Srinakharinwirot University (Ref. SWUEC-097/2563).

In the process of the cervical specimen measurement, the probe was put on the surface of the cervical specimens (Fig. 8). Pressure was applied to ensure the firm attachment of the electrode tips. For Specimen A which the shape was in a cup shape, the specimen was cut into two halves first for ease of measurement. The probe was located as close as possible to the orifice. The measurement lasted 60 s resulting in 1200 samplings. All samplings were averaged to reduce the measurement noise. The measurement data of 10 kHz and that of 50 kHz were used as the low-frequency and high-frequency

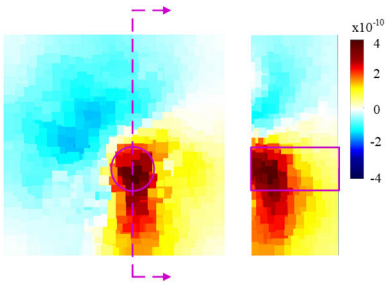

FIGURE 10. The reconstruction images obtained with the WfdEIT method. The left image is the top view and the right image is the side view. The magenta circle (in the left image) and the magenta rectangle (in the right image) indicate the true location of the abnormality.

TABLE 2. Formalin conductivity (S/m).

Freq. (kHz)	Formalin Conductivity (S/m)
2	0.166±0.01
10	0.442±0.02
25	0.616±0.01
50	0.725±0.00
125	0.785±0.01
σ_{10k}-σ_{50k}	-0.283

The values are displayed in the format of the mean±the standard deviation.

TABLE 3. Correction factor of different measurements.

σ(S/m)	10-16: 1-2 [(1)]	8-11: 2-3 [(1)]	9-13: 3-4 [(1)]	11-15: 4-5 [(1)]	13-16: 5-6 [(1)]
0.1	1.086	0.966	1.086	1.085	0.965
0.2	1.084	0.965	1.085	1.084	0.964
0.3	1.084	0.965	1.084	1.083	0.963
0.4	1.083	0.964	1.084	1.083	0.963
0.5	1.083	0.964	1.084	1.083	0.963
Mean	1.084	0.965	1.084	1.084	0.963

[(1)] The display is in the format "Current electrode-Current electrode: Voltage electrode-Voltage electrode".

voltage data, respectively. The selection was based on the SNR performance reported in [26], the SNR at 10 kHz was significantly higher than that of 2 kHz, the current amplitude was also higher, and the SNR at 50 kHz was significantly higher than that of 125 kHz.

III. RESULTS

A. PERFORMANCE OF THE RECONSTRUCTION METHODS

Reconstruction images using the fdEIT and the WfdEIT methods are shown in Fig. 9 and Fig. 10. The abnormality could not be seen with the fdEIT method, but it could be with the WfdEIT method. A positive conductivity change was observed at the region of the abnormality inclusion. The depth of the positive change was ~2-2.5 mm from the measured surface.

B. FORMALIN CONDUCTIVITY

The conductivities of 10% neutral buffered formalin with the developed chamber are shown in Table 2. The conductivity was low at the low frequencies. The difference in conductivity between the selected frequencies mentioned in Section III-D i.e. 10 and 50 kHz was -0.283 S/m.

TABLE 4. Conductivity of the cervical specimens (S/m).

Freq. (kHz)	Reported Normal [6], [9]	Reported CIN2 [6]	Normal Ecto-cervix	Normal TZ	CIN2	Cancer
2	0.051, 0.1	0.336	0.112 ±0.04	0.245± 0.04	0.146± 0.02	0.216± 0.02
10	0.067, 0.17	0.347	0.132 ±0.03	0.262± 0.04	0.168± 0.01	0.236± 0.03
25	0.120, 0.25	0.387	0.158 ±0.02	0.292± 0.03	0.185± 0.01	0.260± 0.03
50	0.213, 0.28	0.442	0.198 ±0.02	0.324± 0.02	0.214± 0.01	0.300± 0.02
125	0.402, 0.40	0.487	0.326 ±0.01	0.494± 0.01	0.328± 0.00	0.443± 0.02
σ_{10k}-σ_{50k}	-0.147, -0.11	-0.095	-0.066	-0.062	-0.046	-0.064

The values are displayed in the format of the mean±the standard deviation.

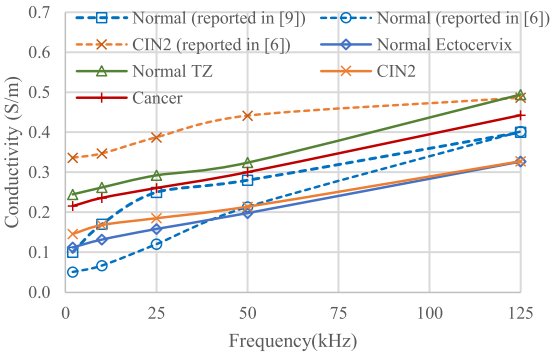

FIGURE 11. The conductivities of the cervical specimens at different cervical parts and different abnormality grades. The bold lines represent the conductivities found in this study and the dashed lines represent the reported conductivities.

C. CORRECTION FACTOR FOR THE CONDUCTIVITY ESTIMATION WITH THE DEVELOPED PROBE

Each chosen measurement for estimating conductivity with the developed probe (mentioned in Section II-A) has its own correction factor α. The correction factors at different tissue conductivities are displayed in Table 3. The correction factors were slightly lower at high simulated conductivities, but not significant (less than 0.3%.) The average values of the factors were approximately 0.964 or 1.084 depending on the measurements.

D. CERVICAL TISSUE CONDUCTIVITY

The conductivities of the cervical specimens in different cervical parts are summarized in Table 4 and Fig. 11. The conductivity of the high frequencies was higher than that of the low frequencies. The conductivity of the transformation zone (TZ) part of the cervical specimens was higher than that of the ectocervix part by 1.5-2.2 times. The conductivity of the CIN2 region, obtained from the hardest specimen (Specimen B), was close to the conductivity of the ectocervix part. Whereas the conductivity of the cancer region, obtained from the softest specimen (Specimen A), was close to that of the TZ part. It is noticeable that the reported conductivity of normal cervices (in vivo) was close to the conductivity of

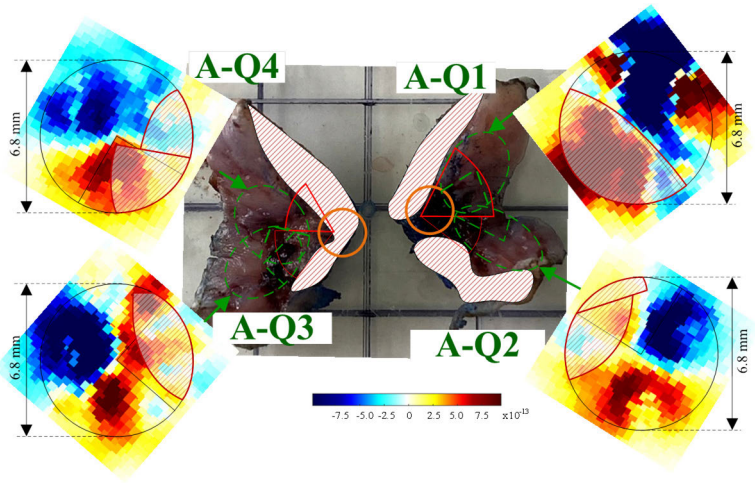

FIGURE 12. Reconstruction images of specimen A. The green circles indicate the measurement locations. The orange circles indicate the rough location of TZ (near the orifice.) The red circular sectors presented on the specimen image and the red pattern-filled areas in the reconstruction images indicate the location of cancer.

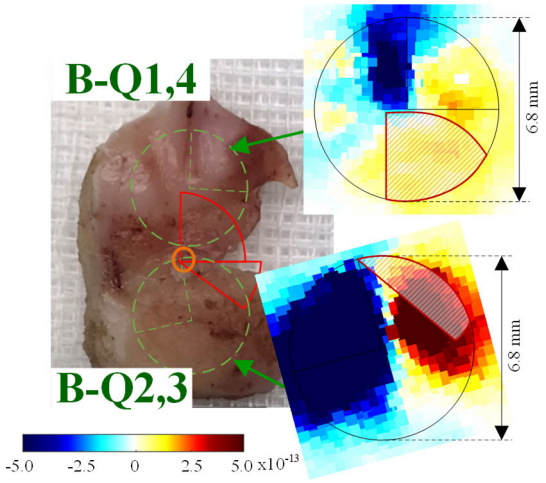

FIGURE 13. Reconstruction images of specimen B. The green circles indicate the measurement locations. The orange circles indicate the rough location of TZ (near the orifice.) The red circular sectors presented on the specimen image and the red pattern-filled areas in the reconstruction images indicate the location of CIN2.

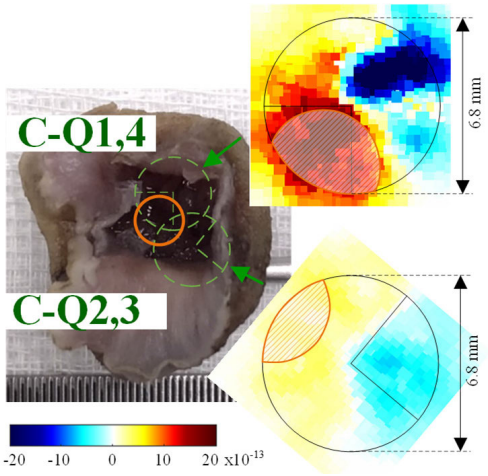

FIGURE 14. Reconstruction images of specimen C. The green circles indicate the measurement locations. The orange circles and the orange pattern-filled areas in the reconstruction images indicate the rough location of TZ (near the orifice).

the ectocervix found in this study. Meanwhile, the reported conductivity of CIN2 cervices was close to the conductivity of the cancer region in this study.

E. RECONSTRUCTION IMAGES OF CERVICAL SPECIMENS

The reconstruction images of the cervical specimens, created by the WfdEIT method, are exhibited in Fig. 12-Fig.14. The summary of the localization performance is also illustrated in Table 5. In the case of Specimen A, in general, the cancer could be localized the cancer with positive changes in conductivity. The cancer location was clearly revealed in the A-Q1 section where the cancer spreading was almost the half region of the measurement area. The cancer could be partly detected in the A-Q2, A-Q3, and A-Q4 sections. However, irrelevant positive change was found in the non-cancer regions in the case of the A-Q2 and A-Q3.

In the case of Specimen B, CIN2 could be localized for all sections, but some irrelevant positive change was found in the B-Q1,4 section. Noticeably, the amplitude of the change in the B-Q2,3 section was significantly larger than that of the B-Q1,4 section. In the case of Specimen C which was the healthy specimen, the positive conductivity change belonged to the region of the TZ part. It is also noticeable that the amplitude of the change was even larger than that of the images of Specimen B (the CIN2 case, hard specimen), but close to that of the images of Specimen A (the cancer case, soft specimen).

TABLE 5. Summary of localization performance.

Specimen section	Localization Result
A-Q1	Success in localizing the cancer
A-Q2	Failure to localize the cancer
A-Q3	Success in localizing the cancer with some concerns
A-Q4	Success in localizing the cancer with some concerns
B-Q1,4	Success in localizing the CIN2 with some concerns
B-Q2,3	Success in localizing the CIN2
C-Q1,4	Success in localizing the TZ region
C-Q2,3	Success in localizing the TZ region

IV. DISCUSSION

A. CONDUCTIVITY OF THE CERVICAL SPECIMENS

An electrode probe was used for estimating the tissue conductivities in this study. The electrodes were attached to the surface of the specimens, without piercing into the specimen matter (non-destructive), and therefore, with this measurement configuration, the conductivity could not be straightforwardly estimated by dividing the measured voltage with the injected current. This is different from the estimation for formalin conductivity that could be measured in a chamber due to its liquid form. The conductivity estimation based on the surface measurement was proposed in [19] and [27]. However, since the diameter of the electrode tips used in this study was large compared to the electrode distances and also the electrode alignment was not in a perfectly straight line, the correction factor was then added to the estimation. The simulation result showed that, with the proposed electrode layout, when the current injection electrodes were placed apart at 54 degrees (e.g. Electrode#8 and #11), the correction factor was 0.965. However, it was 1.084 with the current injection electrodes were placed at 72 degrees apart (e.g. Electrode#10 and #16.) It is worth mentioning that the conductivity estimation in the previous studies ([6], [8], [9], [12], [13], [14], [15]) did not clearly explain how to calculate the conductivity. References [6] and [12] mentioned that the estimation was based on the proportion of the measurement voltage and the injected current, however, the electrode size and the electrode distance were not taken into account. Furthermore, the electrode alignment was not in a straight line but it was aligned in the least sensitive pattern. This may indicate a certain estimation error in the reported conductivities.

The size of the probe developed in this study was comparable to the reported probes used for similar purposes as the summary in Table 6. The diameter of the electrode array was 6.8 mm, while it was 5.5 mm in [6] and [12] (used for in vivo screening of the abnormality in cervices), 5.5-12 mm in [9] and [15] (used for determining the preterm of pregnancy and the outcome of induced labor), or 7-10 mm in [13] and [14] (used for determining the conductivity of tissues). The array size of 5-7 mm could be sufficiently large when compared with the ordinary size of cervical specimens which was approximately 12-15 mm in diameter (with the orifice in the center.) The size of the cervical specimens could be determined as the target measurement region of the cervix

TABLE 6. The summary of reported probe systems.

Probe system	Can be used for Estimating Conductivity	Can be used for Imaging	Have been Implemented on Humans or Specimens
[6] [12] [8]: 4-electrode system with 5.5 mm tip diameter, 4·8 kHz and 614 kHz, 10-20 $uA_{peak-peak}$	Yes	No	In vivo women
[9]: 4-electrode system with 3-12 mm tip diameter, 76-625 kHz, 3-12.5 μA_{peak}	Yes	No	In vivo women
[15]: 8-electrode system with 5.5 mm tip diameter, 76.3 Hz - 625 kHz	Yes	Possibly (not reported)	In vivo women
[13]: 16-electrode system with 7 mm tip diameter, 1 - 100 kHz, 85-310 µA	Yes	Possibly (not reported)	Only implemented in a phantom situation
[14]: 16-electrode system with 10 mm tip diameter, 100 Hz - 500 kHz	Yes	Possibly (not reported)	Implemented on other tissues
[16]: 16-electrode system with 17.5 mm tip diameter, 2 - 125 kHz, 100-800 µA	Yes	Yes (fdEIT)	Only implemented in a phantom situation
[19]: 7-electrode system with 3 mm tip diameter, 2 - 125 kHz, 50-400 µA	Yes	Yes (tdEIT)	Only implemented in a phantom situation
This study: 16-electrode system with 6.8 mm tip diameter, 2 - 125 kHz, 50-400 µA	Yes	Yes (fdEIT0	Cervical specimens

The studies that are based on simulation will not be displayed here.

in the case of in vivo measurement as well. The number of measurements with the probe was then approximately four times to cover most cervix surface. However, the number of in vivo measurements was reported to be eight in [6] and [12] indicating that overlapping regions could exist or the measuring area in the vivo case could be larger than the size of ordinary specimens. Furthermore, the measured regions could be the endocervix, the ectocervix, or the transformation zone part where the cell morphology is different. Conducting measurements without determining the part of the cervix could then result in a large variation of conductivity and cause difficulties in distinguishing normal and abnormal cervices.

The conductivity in different cervical parts of cervical specimens was investigated in this study. Discrepancy in conductivity was found among the reported conductivities including those found in this study. The conductivities of normal ectocervix found in this study were higher than those reported in [6] (based on the eight-location measurement and used the proportion of voltage and current for computing the conductivity) by 1.4-2.2 times at 25 kHz and below, but they were lower by 7-19% at 50-125 kHz. Meanwhile, the conductivities of the ectocervical part found in this study were lower than those reported in [9] by 18-37% at 10 kHz and higher (however, the method to compute the conductivity was not

provided.) Furthermore, the conductivities of the CIN2 region found in this study were significantly lower i.e. 33-57% than those reported in [6]. The conductivity discrepancy could be relevant to the conductivity estimation methods. For example, in the case of estimating with a chamber, the conductivity of abnormal cervical tissues at 10 kHz was 166 times higher than that of normal tissues [7]. However, when estimating with a probe, the conductivity difference was only 1.6 times reported in [6] and 1.3 times found in this study. The discrepancy involves the measurement site on the cervix. The conductivity of normal cervices in the previous studies could be the average of the conductivity of the different cervical parts that have different cell morphology. Careful selection of the measurement site and the cervical parts should then be conducted to obtain an accurate conductivity value.

References [6], [12], and [8] reported that the conductivity of the high grades of abnormality (CIN2 and CIN3) was higher than that of the lower grade (CIN1) and this is consistent with what was found in this study. The conductivity of the cancer region was also found that 1.4 times higher than that of the CIN2 region. However, surprisingly, the conductivity of the tissue in the TZ part was found highest among that of the other cervical parts and even that of the CIN2 region. The conductivity of the TZ part was very close to that of the cancer region. The morphology of the TZ's cells which are a combination of columnar cells are squamous cells and that of the cancer cells which are generally cuboidal or columnar [1] are similar and result in high conductivity for both of them. This could be also observable during the gross examination of specimens since the TZ parts and the cancer region were generally softer than the other regions. Since the cervical abnormality tends to originate at the TZ part [30], it will be difficult to detect the abnormality with conductivity measurement if the abnormality resides only in the TZ part. Additionally, [6] reported that the conductivity difference between normal cervices (or the normal ectocervix in this study) and the CIN2 cervices became smaller at the high frequencies, however, this did not comply with the difference between the conductivity of the normal TZ parts and the cancer region. It is also worth noting that Specimen B had a small exposed region of the TZ part and the CIN2 region had already spread into the region of the ectocervix. This situation is beneficial for reconstruction. The formalin fixation could only slightly (or not) affect the conductivity estimation in this study since the fixation time was limited to only four hours. Furthermore, the measured conductivities of cervical specimens were significantly different from the conductivity of formalin ($\sim$3 times smaller.)

B. RECONSTRUCTION IMAGES OF THE CERVICAL SPECIMENS

The volume of the investigated specimens in this study was considerably smaller and the volume of the abnormality was even smaller. Compared to similar studies, [25] (measured with a well-plate and with a 16-electrode configuration), [16] (measured with a planar electrode plate and with a 16-electrode configuration), and [19] (measured with a probe and with a 7-electrode configuration) proposed systems to image the conductivity distribution in a small volume as well. The size of the electrode array in this study was 2.2-2.9 times smaller than most of the probes used in the previous studies i.e. [16], [25], but only a half compared to [19] and [25] achieved to implement frequency difference reconstruction for monitoring cell-loaded hydrogel in a liquid-filled well, however, the hydrogel inclusion needing to image was large i.e. one-fourth of the volume. The large probe system proposed in [16]. Even though it had shown successful reconstruction with the frequency difference method, it is not practical for measuring with real cervical specimens since the specimens could be in a cup or a cone shape, rather than a flat shape (this work was also based on simulation.) In the case of the probe system proposed in [19], the size of the electrode array was only 3 mm in diameter and it could be too small. Furthermore, it had not been implemented with a frequency difference setting as well. The proposed 6.8 mm-diameter electrode array (in a 16-electrode configuration) in this study is suitable compared to the size of cervical specimens i.e. 12-15 mm in diameter. The number of measurements of 2-4 times could cover the most regions of specimens. The array size was also similar to [14] (containing 8 electrodes with 7 mm in diameter of the electrode array), but it has not been used for imaging in this cervix application. Actually, the size of 5.5 mm in diameter proposed in [6], [8], [9], [12], and [15] seems suitable as well, but most of them had only four electrodes that are unsuitable to use for image reconstruction. Only the probe in [15] could be used since it contained eight electrodes. The probe proposed in [13] could be too large (10 mm in diameter) when considering that the orifice is in the center of the specimens. Note that the probes proposed in [13] and [15] have not been used for imaging with the cervix to date.

Even though reconstruction with the fdEIT method was reported could be used for localized abnormality in medical applications [16], [23], the simulation found that it could not used with the cervix situation. This is possibly due to the small volume and the larger difference in conductivity of the low and the high frequencies of normal cervices compared to that of abnormal cervices ($\sim$1.5 times.) Projection is then necessary in this case resulting in the WfdEIT method succeeding in the localization (in the simulation scenario.) The positive conductivity change was observed since the difference in conductivity of normal cervices was -0.147 S.m, but it was -0.095 S/m for that of abnormal cervices i.e. lesser negative. However, small artifacts were still observable even though the simulation was noiseless.

The abnormalities in the specimens were able to be localized in most cases. For the specimen case of CIN2, the abnormality was clear to address due to the small region of the TZ part. The TZ part became troublesome since the electrical property was similar to that of the cancer region

as mentioned in Section IV-A. The conductivity change in the reconstruction images in the region of the TZ part and the cancer showed the same positive change and this caused difficulty in distinguishing the cancer from the TZ tissue. In the case of the normal cervical specimen, the positive change was also observable, but this change belonged to the TZ part rather than the cancer. This observation supports the statement mentioned in Section IV-A and then the site to measure the conductivity or to reconstruct must be a crucial concern. Measuring the conductivity at the TZ part could lead to misinterpretation in the presence of abnormality.

The artifacts in the images could be caused by difficulties in the measurement process. This involved the curve of the specimens and the uneven thicknesses at different measurement sites. The softness at measurement sites was also an issue of concern. The tip of some electrode pins could be easily buried with the surrounding tissue at the very soft sites of the cervix surface and this led to a complicated current pathway. This could explain the poorer performance of the case of Specimen A where the tissue was very soft at the TZ part and the cancer region compared to the other cases. The pressure applied to the probe could be relevant as well. This could introduce the different amplitude in the images.

The image of conductivity distribution found in this study could be used to help pathologists in the process of sectioning LEEP specimens. Furthermore, the image is also beneficial for obtaining prediagnosis information, particularly for determining the spread of abnormality. However, since the conductivity change in the TZ part is similar to the change in the abnormality region, the image interpretation in the TZ region still needs to do with care. It is worth noting that implementing the probe in vivo with women could be possible as well. Physiologists will have several benefits in determining the necessity for a cervix biopsy.

V. CONCLUSION

In this work, the reconstruction images of cervical specimens were constructed with the frequency-difference EIT technique. An electrode probe was developed for this reconstruction purpose and also for measuring the conductivity. Experimental results found that the conductivity of the ectocervix was the smallest compared to the abnormal cervical regions and the tissue in the transformation zone (TZ) part. The conductivity of the CIN2 region was smaller than that of the cancer region and the TZ part. The frequency spectrum of conductivity of the TZ part and that of the cancer region, however, was very similar. The weighted-frequency difference EIT method was found to be suitable for imaging the cervical abnormality. The abnormality could be localized in most cases as positive conductivity changes. However, due to the similarity of the tissue in the TZ part and the cancer region, the conductivity change in the reconstruction images in the TZ region was also the same i.e. positive conductivity changes and this caused difficulties in distinguishing the normal tissue in the TZ part from the cancer. The measurement site is then required to be selected with care or the region of the TZ part should be investigated and addressed during the measurement as well.

REFERENCES

[1] J. Lu, Z. Xu, F. Jiang, Y. Wang, Y. Hou, C. Wang, and Q. Chen, "Primary clear cell adenocarcinoma of the bladder with recurrence: A case report and literature review," *World J. Surgical Oncol.*, vol. 10, no. 1, pp. 1–6, Dec. 2012.

[2] R. Vidya and G. M. Nasira, "A pioneering cervical cancer prediction prototype in medical data mining using clustering pattern," *Int. J. Data Mining Techn. Appl.*, vol. 4, no. 2, pp. 63–66, Dec. 2015.

[3] K. Nam, "Colposcopy at a turning point," *Obstetrics Gynecology Sci.*, vol. 61, no. 1, p. 1, 2018.

[4] N. Shanmugapriya and P. Devika, "Comparing the effectiveness of liquid based cytology with conventional PAP smear and colposcopy in screening for cervical cancer and it's correlation with histopathological examination: A prospective study," *Int. J. Reproduction, Contraception, Obstetrics Gynecol.*, vol. 6, no. 12, pp. 5336–5340, 2017.

[5] G. Yin, J. Li, A. Wu, J. Liang, and Z. Yuan, "Four categories of LEEP for CIN of various areas: A retrospective cohort study," *Minimally Invasive Therapy Allied Technol.*, vol. 26, no. 2, pp. 104–110, Mar. 2017.

[6] B. H. Brown, J. A. Tidy, K. Boston, A. D. Blackett, R. H. Smallwood, and F. Sharp, "Relation between tissue structure and imposed electrical current flow in cervical neoplasia," *Lancet*, vol. 355, no. 9207, pp. 892–895, Mar. 2000.

[7] L. Das, S. Das, and J. Chatterjee, "Electrical bioimpedance analysis: A new method in cervical cancer screening," *J. Med. Eng.*, vol. 2015, pp. 1–5, Feb. 2015.

[8] S. Abdul, B. H. Brown, P. Milnes, and J. A. Tidy, "A clinical study of the use of impedance spectroscopy in the detection of cervical intraepithelial neoplasia (CIN)," *Gynecologic Oncol.*, vol. 99, no. 3, pp. S64–S66, Dec. 2005.

[9] R. P. Jokhi, B. H. Brown, and D. O. Anumba, "The role of cervical electrical impedance spectroscopy in the prediction of the course and outcome of induced labour," *BMC Pregnancy Childbirth*, vol. 9, no. 40, pp. 1–8, Dec. 2009.

[10] T. Ouypornkochagorn, B. Phiboon, S. Wongkhamhan, P. Pikulkeaw, and W. Kraisuwan, "Monitoring porosity and swelling ratio of scaffolds with electrical conductivity," *IEEE Trans. Instrum. Meas.*, vol. 73, pp. 1–11, 2024.

[11] S. Leonhardt, A. Cordes, H. Plewa, R. Pikkemaat, I. Soljanik, K. Moehring, H. J. Gerner, and R. Rupp, "Electric impedance tomography for monitoring volume and size of the urinary bladder," *Biomedizinische Technik/Biomedical Eng.*, vol. 56, no. 6, pp. 301–307, Jan. 2011.

[12] B. H. Brown, P. Milnes, S. Abdul, and J. A. Tidy, "Detection of cervical intraepithelial neoplasia using impedance spectroscopy: A prospective study," *BJOG, Int. J. Obstetrics Gynaecology*, vol. 112, no. 6, pp. 802–806, Jun. 2005.

[13] T. Zhang, Y. Jeong, D. Park, and T. Oh, "Performance evaluation of multiple electrodes based electrical impedance spectroscopic probe for screening of cervical intraepithelial neoplasia," *Electronics*, vol. 10, no. 16, p. 1933, Aug. 2021.

[14] B. Karki, H. Wi, A. McEwan, H. Kwon, T. I. Oh, E. J. Woo, and J. K. Seo, "Evaluation of a multi-electrode bioimpedance spectroscopy tensor probe to detect the anisotropic conductivity spectra of biological tissues," *Meas. Sci. Technol.*, vol. 25, no. 7, Jul. 2014, Art. no. 075702.

[15] D. O. C. Anumba, V. Stern, J. T. Healey, S. Dixon, and B. H. Brown, "Value of cervical electrical impedance spectroscopy to predict spontaneous preterm delivery in asymptomatic women: The ECCLIPPx prospective cohort study," *Ultrasound Obstetrics Gynecology*, vol. 58, no. 2, pp. 293–302, Aug. 2021.

[16] T. Ouypornkochagorn, N. Ngamdi, S. Ouypornkochagorn, and T. Trongwongsa, "Cervical intraepithelial neoplasia localization with frequency-difference electrical impedance tomography—Simulation and phantom study," *IEEE Access*, vol. 11, pp. 67745–67754, 2023.

[17] T. K. D. S. Saito, R. A. Pedriali, C. M. Gabella, M. C. Junior, and E. J. Leonardo, "Preliminary results of cervical impedance measurements," *Res. Biomed. Eng.*, vol. 34, no. 2, pp. 110–114, May 2018.

[18] A. Sillaparaya and T. Ouypornkochagorn, "Planar electrode configurations of electrode plates for the localization of cervical abnormality based on electrical impedance tomography (EIT)—A simulation study," in *Proc. 11th Int. Conf. Biomed. Eng. Technol.*, Tokyo, Japan, Mar. 2021, pp. 27–33.

[19] N. Ngamdi, J. Sriwilai, T. Trongwongsa, and T. Ouypornkochagorn, "A development of electrode probes for imaging precancerous lesions with electrical impedance tomography technique: A phantom study," *J. Appl. Sci. Eng.*, vol. 27, no. 1, pp. 1901–1910, 2023.
[20] I. Frerichs, M. B. P. Amato, A. H. van Kaam, D. G. Tingay, Z. Zhao, B. Grychtol, M. Bodenstein, H. Gagnon, S. H. Böhm, E. Teschner, O. Stenqvist, T. Mauri, V. Torsani, L. Camporota, A. Schibler, G. K. Wolf, D. Gommers, S. Leonhardt, and A. Adler, "Chest electrical impedance tomography examination, data analysis, terminology, clinical use and recommendations: Consensus statement of the translational EIT development study group," *Thorax*, vol. 72, no. 1, pp. 83–93, Jan. 2017.
[21] T. Ouypornkochagorn, N. Terzija, P. Wright, J. L. Davidson, N. Polydorides, and H. McCann, "Scalp-mounted electrical impedance tomography of cerebral hemodynamics," *IEEE Sensors J.*, vol. 22, no. 5, pp. 4569–4580, Mar. 2022.
[22] E. Malone, G. S. dos Santos, D. Holder, and S. Arridge, "Multifrequency electrical impedance tomography using spectral constraints," *IEEE Trans. Med. Imag.*, vol. 33, no. 2, pp. 340–350, Feb. 2014.
[23] T. Ouypornkochagorn, N. Polydorides, and H. McCann, "Towards continuous EIT monitoring for hemorrhagic stroke patients," *Frontiers Physiol.*, vol. 14, pp. 1–9, Apr. 2023.
[24] S. C. Jun, J. Kuen, J. Lee, E. J. Woo, D. Holder, and J. K. Seo, "Frequency-difference EIT (fdEIT) using weighted difference and equivalent homogeneous admittivity: Validation by simulation and tank experiment," *Physiological Meas.*, vol. 30, no. 10, pp. 1087–1099, Oct. 2009.
[25] H. Wu, W. Zhou, Y. Yang, J. Jia, and P. Bagnaninchi, "Exploring the potential of electrical impedance tomography for tissue engineering applications," *Materials*, vol. 11, no. 930, pp. 2–11, 2018.
[26] T. Ouypornkochagorn and N. Ngamdi, "High-precision electrical impedance tomography system using package excitation," *IEEE Trans. Instrum. Meas.*, vol. 72, pp. 1–11, 2023, doi: 10.1109/TIM.2023.3324360.
[27] D. Schroder, *Semiconductor Material and Device Characterization*. Hoboken, NJ, USA: Wiley-IEEE Press, 2006.
[28] N. Polydorides, W. R. B. Lionheart, and H. McCann, "Krylov subspace iterative techniques: On the detection of brain activity with electrical impedance tomography," *IEEE Trans. Med. Imag.*, vol. 21, no. 6, pp. 596–603, Jun. 2002.
[29] N. Polydorides and W. R. B. Lionheart, "A MATLAB toolkit for three-dimensional electrical impedance tomography: A contribution to the electrical impedance and diffuse optical reconstruction software project," *Meas. Sci. Technol.*, vol. 13, no. 12, pp. 1871–1883, Dec. 2002.
[30] H. Deng, E. Hillpot, S. Mondal, K. K. Khurana, and C. D. Woodworth, "HPV16-immortalized cells from human transformation zone and endocervix are more dysplastic than ectocervical cells in organotypic culture," *Sci. Rep.*, vol. 8, no. 1, pp. 1–13, Oct. 2018.

TAWEECHAI OUYPORNKOCHAGORN (Senior Member, IEEE) received the B.Eng. degree in electrical engineering from the King Mongkut's University of Technology Thonburi, Thailand, in 1998, the M.Eng. degree in computer engineering from Kasetsart University, Thailand, in 2003, and the Ph.D. degree in engineering from the University of Edinburgh, U.K., in 2016. He is currently a Lecturer with Srinakharinwirot University, Thailand, researching electrical impedance tomography (EIT) in medical applications, bioimpedance analysis, medical instrumentation, and applications using artificial neural networks.

NAPATSAWAN NGAMDI received the B.Eng. and M.Eng degrees in biomedical engineering from Srinakharinwirot University, Thailand, in 2022 and 2023. Her specialty is related to electrical impedance tomography (EIT) in medical applications.

SAIROONG OUYPORNKOCHAGORN received the B.Sc. degree in chemistry and the M.Sc. degree in applied analytical and inorganic chemistry from Mahidol University, Thailand, and the Ph.D. degree in analytical chemistry from the University of Aberdeen, U.K. She is currently a Lecturer with Naresuan University, Thailand, researching analytical and liquid chromatography in various applications.

JARUWAN SRIWILAI received the Bachelor of Science degree in applied biology from Songkhla Rajabhat University, Thailand, in 2006. She is a Pathologist Assistant at H. R. H. Maha Chakri Sirindhorn Medical Center, Nakhon Nayok, and also with the Department of Pathology, Faculty of Medicine, Srinakharinwirot University, Bangkok, Thailand. Her research interest includes cytotechnology.

THERDKIAT TRONGWONGSA received the Doctor of Medicine (M.D.) degree from the Faculty of Medicine, Srinakharinwirot University, Thailand, in 2009, the Diploma degree from the Thai Board of Anatomical Pathology, Faculty of Medicine Siriraj Hospital, Mahidol University, Thailand, in 2012, and the Diploma degree from the Thai Board of Hematopathology, in 2019. He is currently a Lecturer with Srinakharinwirot University and a Pathologist with the H. R. H. Maha Chakri Sirindhorn Medical Center, Nakhon Nayok, Thailand. His research interests include general anatomical pathology and hematopathology.